



First results from the equatorial geomagnetic station at Entoto Observatory and Research Center

Amoré Nel¹, Nigussie Giday², Marcos Da Silva³, Daniel Chekole², Jürgen Matzka³, Ziyaad Isaacs¹, Oliver Bronkala³, and Lamessa Mogasa²

Correspondence: Amoré Nel (anel@sansa.org.za)

- 2 Abstract. This paper presents the initial results from the newly deployed Entoto Magnetometer Station near Addis Ababa,
- 3 Ethiopia, a collaborative project involving the South African National Space Agency (SANSA), the Space Science and Geospa-
- 4 tial Institute (SSGI) in Ethiopia, and the German Centre for Geosciences (GFZ). The station, equipped with a LEMI-025 flux-
- 5 gate magnetometer and a GSM-90 Overhauser sensor, aims to monitor geomagnetic field variations and enhance space weather
- 6 research in the African sector. This deployment is a significant step in SANSA's efforts to establish a comprehensive geomag-
- 7 netic network across Africa, contributing to global space weather models. This is of particular importance, as the ENTOTO
- 8 station is, to our knowledge, the only currently operational magnetic observatory near the dip equator in the African region,
- 9 positioning the ENTOTO Observatory and Research Center at SSGI as a key contributor to regional and global geomagnetic
- 10 research. Early observations show a good characterization of geomagnetic disturbances, with observed field changes align-
- 11 ing closely with the Dst index variations, which has important implications for space weather forecasting. The station also
- 12 generates local K-index data for this region, providing valuable insights into ionospheric variability and its effects on techno-
- 13 logical systems. This paper details the station's setup, data processing methodologies, and initial scientific results, laying the
- 14 foundation for future research and collaboration in this critical area of space science.

15 1 Introduction

- 16 The Earth's magnetic field plays a crucial role in shielding the planet from solar radiation and influencing space weather
- 17 (Kamide, 2001; Kotzé et al., 2015). Generated primarily by the geodynamo in the Earth's liquid core, this field extends from
- 18 the core through the planet's surface into space, where it interacts with solar wind and cosmic radiation. Other contributing
- 19 sources include electrical currents in the ionosphere and magnetosphere, magnetized crustal rocks, and induced currents in the
- 20 mantle and oceans. These internal and external sources collectively shape the geomagnetic field. Secular variation, the slow
- 21 temporal change in the magnetic field, provides insight into the geodynamo's behavior, making long-term monitoring essential
- 22 for understanding natural processes and the technological impacts of space weather (Nel et al., 2024).
- 23 Ground-based geomagnetic observatories are vital for monitoring these variations. High-quality data from observatories have

¹South African National Space Agency (SANSA), South Africa

²Department of Space and Planetary Science, Space Science and Geospatial Institute (SSGI), Addis Ababa, Ethiopia

³GFZ German Research Centre for Geosciences, Potsdam, Germany



54 55

56

57



been instrumental in studying secular variation and disturbances such as geomagnetic storms (Matzka et al., 2010; Nel and 24 25 Kotzé, 2024). Despite their importance, the global network of observatories faces challenges, particularly in under-monitored 26 regions like Africa and the Southern Hemisphere (Giday et al., 2020; Yizengaw and Moldwin, 2009). The scarcity of observa-27 tions in these areas underscores the need for new stations, especially near the magnetic equator, where space weather strongly influences the ionosphere (Mungufeni et al., 2018; Macmillan, 2007). The establishment of the Entoto Magnetometer Station 28 29 in Ethiopia addresses this gap. Located near the magnetic equator, the station is part of SANSA's broader efforts to improve regional space weather forecasting. This collaborative initiative between SANSA, Ethiopia's SSGI, and Germany's GFZ, aims to 30 generate high-quality geomagnetic data to fill critical gaps in the global network. By capturing geomagnetic variations specific 31 to the African sector, the Entoto station enhances both regional and global space weather models, contributing to improved 32 predictions of geomagnetic storms and their effects on technological systems, including communication networks and power 33 grids (Matzka et al., 2010). 34

Several research fields are essential for understanding geomagnetic phenomena, particularly near the magnetic equator. Among these are studies of the equatorial ionosphere, equatorial plasma bubbles (Giday et al., 2020), geomagnetic storms, solar quiet (Sq) variations, the Equatorial Electrojet (EEJ), and the counter-equatorial electrojet (Habarulema et al., 2019). The EEJ, in particular, is of significant interest as it represents a concentrated eastward electric current superimposed on the global Sq current system. The relationship between the global Sq current system and the EEJ remains a subject of active research and ongoing debate (Yamazaki and Maute, 2016). Understanding the interactions between these currents is critical for improving models of ionospheric conductivity, geomagnetic variations, and space weather impacts on equatorial regions.

Despite the importance of such studies, Africa faces a persistent challenge due to the lack of active magnetometer stations along the magnetic equator. Currently, there are no operational magnetometer stations in the region with the necessary capabilities to effectively study Sq variations and the EEJ. Existing networks, such as the MAGnetic Data Acquisition System (MAGDAS) and the International Real-time Magnetic Observatory Network (INTERMAGNET), include a limited number of stations in Africa, but many are either inactive or positioned at latitudes too far from the equator to capture equatorial phenomena accurately.

For instance, INTERMAGNET operates three observatories in northern Africa: one in Ethiopia, one in Mbour, Senegal, and one in Tamanrasset, Algeria. However, both the Ethiopian and Senegalese stations have ceased recording data, and the Algerian station is located too far from the magnetic equator to be useful for equatorial studies. Similarly, the MAGDAS and African Meridian B-Field Education and Research (AMBER) networks, which previously had several stations along the magnetic equator, have experienced prolonged inactivity. As a result, Ethiopia currently lacks a functioning pair of low-latitude and equatorial stations, both of which are crucial for accurately studying EEJ dynamics and Sq variations.

The scarcity of operational equatorial magnetometer stations in Africa presents a major obstacle to advancing geomagnetic and space weather research in the region. Without high-resolution, continuous ground-based observations, researchers must rely on satellite data, which, while valuable, lacks the temporal resolution necessary for detailed EEJ and Sq variation analysis.



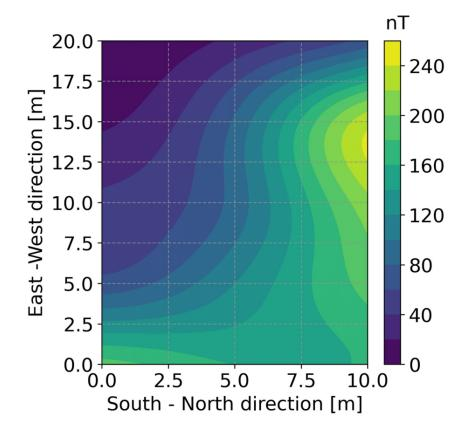


Figure 1. A magnetic gradient survey was conducted within the original section of the Entoto observatory in the North-Western sector $(9^{\circ}06^{'}33.6"N, 8^{\circ}48'24.1"E)$.

Additionally, the absence of equatorial ground-based measurements limits the ability to validate global geomagnetic models and weakens Africa's contribution to international space weather monitoring efforts.

The establishment of the Entoto Magnetometer Station represents a significant step toward addressing this gap. By providing high-frequency geomagnetic measurements from a location near the magnetic equator, the station enables in-depth investigations of the EEJ, Sq variations, and their interactions with global and regional space weather phenomena. The station's data will contribute to both regional forecasting and global geomagnetic modeling, enhancing our understanding of equatorial electrodynamics and their impact on communication, navigation, and power systems. This will improve the monitoring and prediction of space weather phenomena in Africa, especially in regions historically underrepresented in existing networks (Uemoto et al., 2010).

The local K-index, derived from ground-based measurements, is an essential tool for assessing local disturbance monitoring and prediction. Numerous space weather prediction centers have started measuring their local K-index using local magnetometer station data, in order to do regional forecasting: Unlike the planetary Kp-index, which averages data from multiple







Figure 2. Magnetometer Setup: The magnetometer is housed in a protective structure designed to withstand environmental challenges, including potential flooding, and to maintain temperature stability. Data is logged continuously and transferred to the respective institutes for analysis and storage.

observatories worldwide, the local K-index provides region-specific insights into geomagnetic activity. For stations located near the magnetic equator, such as Entoto, the K-index must account for the unique influence of the equatorial electrojet, which can distort the magnetic field measurements used to compute the index. Recent studies, such as those conducted at the Phuket station in Thailand, have demonstrated the importance of selecting appropriate calibration values for generating accurate local K-indices in equatorial regions (Hamid et al., 2014; Myint et al., 2022). One of the key challenges in computing the local K-index near the equator is determining the lower limit (L₉) for the K-index scale, which varies with geomagnetic latitude. Equatorial stations require higher L₉ values due to the strong influence of the EEJ, which can otherwise lead to an overestimation of geomagnetic disturbances. At the Entoto station, the analysis of the local K-index will provide critical insights into the day-to-day variability of the EEJ and its impact on geomagnetic activity. By generating accurate local K-indices, the station will enhance regional space weather prediction capabilities, particularly in terms of forecasting geomagnetic storms that could disrupt communication systems and power grids. Additionally, the data collected at Entoto will contribute to a broader understanding of how geomagnetic disturbances evolve in the African sector, filling a critical gap in the global geomagnetic observation network (Menvielle et al., 1995).

The establishment of the Entoto magnetometer station marks a significant milestone in the advancement of geomagnetic research in Africa. By providing high-quality data on the local K-index and geomagnetic field variations, the station will play





85 a pivotal role in improving space weather prediction capabilities both regionally and globally. The collaboration between

86 SANSA, the SSGI, and the GFZ highlights the importance of regional efforts in addressing the global challenges posed by

87 space weather.

88

2 Site Selection and Instrumentation

A geomagnetic observatory is where the geomagnetic field vector is recorded continuously over a long period of time (Matzka 89 et al., 2010). Ideally, the site should be free from any static disturbances caused by local anomalies, as well as far away from 90 human traffic that could cause temporal disturbances. The Entoto Observatory, established in 2014, one of the facilities of 91 the then Ethiopian Space Science and Technology Institute (now Space Science and Geospatial Institute (SSGI)), represents 92 93 a key step in advancing the nation's space science research. Funded by the Ethiopian government, along with support from universities, international partners, and private donors, the observatory offers the necessary facilities for research in space 94 95 science, geospatial technologies, and astronomy. Located at the highest point in Addis Ababa, at an elevation of 3200 metres above sea level, it reflects SSGI's commitment to research and positions Ethiopia as a leader in regional and global space 96 science. The Entoto observatory is situated approximately 15 km North-East of Addis Ababa. Its location, away from local 97 settlements and adjacent Entoto national park, ensures minimal interference from local magnetic noise and provides stable 98 99 environmental conditions for long-term monitoring. A magnetic gradient survey was conducted (see Figure 1) and a deployment site identified within the original section of the Entoto observatory in the North-Western sector $(9^{\circ}06^{'}33.6" N, 38^{\circ}48^{'}24.1" E)$. 100 It is about 20 meters from the western perimeter fence, and 15 meters from an abandoned hut. 101

The protective structure for the proposed magnetometer station is based on the design of SANSA's protective structure at our INTERMAGNET observatory in Keetmanshoop (KMH). Some adjustments were made to this structure, for example, to compensate for potential flooding which could occur in Addis Ababa. The original structure was designed to be buried underground, the new structure will be above ground, with ample area underneath the floor for sudden water flow. Better venting pipes were designed for temperature stability. In partnership with the GFZ, a converter program for the LEMI magnetometer data recorder has been written. The LEMI-025 is connected via RS232 to a Linux PC and the binary data is converted to

108 readable ASCII format. The bias signals and DAC values will be monitored and checked for any anomalies.

The Entoto magnetometer station is equipped with a GSM-90 Overhauser sensor and a LEMI-025 fluxgate magnetometer. 109 The GSM-90 is a portable Overhauser magnetometer that measures the total magnetic field strength with high accuracy. Its 110 application varies, but for this project it's implemented for long term observatory use and will measure the scalar signal of 111 the local geomagnetic field. The LEMI-025 is an extremely sensitive 3-axis fluxgate magnetometer (FGM) that measures the 112 3 components of the geomagnetic field (thus provides directional information) and its variation at 1-second resolution. The 113 LEMI-025 was placed on a magnetometer pillar within the protective structure and the GSM-90 Overhauser a few metres from 114 115 the structure (see Figure 2) and further adjustments and testing will ensue, e.g., looking for reasonable variations, timestamps, adjusting the placement of the instruments, checking for disturbances in the serial line etc. With this dual magnetometer setup 116 one can obtain both the total strength and direction of the local magnetic field, and enables a more complete understanding 117



118

126

127



combining these two sensors it provides both precision and detailed time series data. When studying space weather phenomena, both the intensity and the direction of the geomagnetic field changes are crucial. Using both instruments at geomagnetic observatories helps to monitor geomagnetic storms, substorms, and ionospheric phenomena effectively.

The sensor house comprises a reinforced structure to protect against environmental challenges. The magnetometer sensor is connected to the control room via a cable, ensuring stable power supply through a power system. The magnetic field is represented by its three components, North (X), East (Y), and vertical (Z), measured with respect to the local geomagnetic coordinate system, with Z being positive downward (Denardini et al., 2015). These components are digitized and logged,

of geomagnetic variations. Although the GSM-90 is highly accurate, it has a lower sampling rate than the LEMI-025, thus

3 Methodology

- The Entoto magnetometer station records variations in the geomagnetic field along the X, Y, and Z components with high temporal resolution. These measurements enable the identification of geomagnetic activity patterns, including responses to solar
- 130 wind disturbances and geomagnetic storms. The collected data undergoes a series of processing steps to extract meaningful
- 131 geophysical signals while mitigating noise and long-term trends. The raw data is sampled at one-minute intervals and stored in
- 132 IAGA-2002 format. Initial testing of the instrumentation was conducted at SANSA's facilities in South Africa before deploy-
- 133 ment in Ethiopia to ensure proper calibration and data integrity.

enabling high temporal resolution analysis for space weather monitoring.

- 134 To isolate external geomagnetic variations, the main field, which mainly originates from the Earth's core, is subtracted using
- the CHAOS 8.2 model (Kloss et al., 2025). This model estimates the internal geomagnetic field at the station's coordinates
- 136 during analysis and is limited to 2025.1 to avoid extrapolation. These estimated values are subtracted from the observed data
- 137 to obtain the corrected geomagnetic field components, removing long-term variations such as secular changes and leaving only
- 138 the external field perturbations. This step ensures that local geomagnetic fluctuations are not influenced by global-scale internal
- 139 variations.
- 140 To study short-term geomagnetic variations, the residual field components undergo further processing. A Butterworth high-
- pass filter with a cutoff period of approximately 72 hours is applied to remove long-term variations. To account for solar quiet
- 142 variations, a quiet-day mean for each month is computed and subtracted from the dataset. Finally, a daily running mean is
- 143 subtracted from the data to eliminate long-period fluctuations. This process isolates daily geomagnetic variations primarily
- influenced by ionospheric and magnetospheric currents, allowing for a more precise analysis of space weather effects.
- 145 To provide a broader context for local geomagnetic disturbances, the planetary Ap index is incorporated into the analysis. The
- 146 maximum daily Ap index values are overlaid on the corrected geomagnetic field plots, with color-coded markers indicating
- 147 active disturbance conditions for Ap values greater than or equal to 19 and geomagnetic storm conditions for Ap values ex-
- 148 ceeding 36. The integration of Ap index data allows for direct comparisons between local fluctuations and global geomagnetic



151



149 activity. This step is essential for correlating regional space weather phenomena with larger-scale geomagnetic disturbances

150 that could impact communication systems and navigation infrastructure.

3.1 Estimating the local K index

152 The K-index quantifies geomagnetic disturbances on a quasi-logarithmic scale from 0 (quiet) to 9 (strong storms). The En-

153 toto station's local K-index is computed using the open-source MagPy software (Stolle et al., 2018) following the Finnish

154 Meteorological Institute (FMI) method, which is widely used in geomagnetic observatories. The International Association of

155 Geomagnetism and Aeronomy (IAGA) has standardized four computer-based K-index algorithms that can be applied glob-

156 ally. These algorithms use different solar regular (SR) curve estimation techniques. Among them, the FMI method proposed

157 by Sucksdorff et al. (1991) is considered the most reliable compared to manual hand-scaling techniques. The FMI method is

158 widely used for K-index generation at various observatories and serves as a baseline method for evaluating newer approaches,

159 such as the nowcast K-index used in space weather forecasting. The FMI method employs a linear elimination approach, using

160 geomagnetic field data from three consecutive days to estimate the SR curve for a given day.

161 The calculation of the local k-index using the FMI method is dependent on a station specific constant, called L₉. This value

represents the threshold geomagnetic range (in nanoTesla) that corresponds to the highest level of activity (K = 9) at that sta-

163 tion. L₉ is not a dynamic variable, but a fixed value that is determined empirically using long-term historical data, typically

164 over several years or a full solar cycle. It reflects the station's geomagnetic latitude and local environmental conditions, such

as the proximity to the local EEJ. It is usually analyzed using the statistical distribution of magnetic ranges to align with global

166 K-index conventions.

While software like MagPy can compute K-indices in realtime, it requires a pre-defined L₉ value to map the observed 3-hour

168 range maxima to the appropriate K-level. For the Entoto station outside Addis Ababa, it is possible to use the historical L₉

value from the now decommissioned INTERMAGNET station AAE, provided that the geomagnetic environment and signal

170 processing are comparable.

171 Derivation of the K-index at the Entoto station begins by importing high-resolution time series raw data at minute inter-

172 vals. A baseline correction is applied and filtering to remove non-geomagnetic noise. The geomagnetic time series is then

segmented into 3-hour windows, and for each interval, the maximum and minimum values of the horizontal field components

are determined to compute the fluctuation range. The thresholds account for the influence of the equatorial electrojet, which

175 can introduce distortions to standard K-index computations. Based on the fluctuation range, MagPy assigns a K-index value

176 between 0 and 9 to each 3-hour period. This approach ensures that the K-index calculated by MagPy is both precise and

station-specific, capturing local geomagnetic disturbances that may affect technological systems or contribute to space weather

178 research.

169

173

174

177

The next few subsections outline the procedures to isolate the equatorial electrojet (EEJ) and magnetospheric contributions

180 from low-latitude ground-based geomagnetic observations. The approach is based on removing internal and large-scale external





- 181 field components from the horisontal magnetic field using the CHAOS 8.2 model, and separating diurnal (ionospheric) and
- 182 nocturnal (magnetospheric) variations.

183 3.2 Data Preparation

- 184 Geomagnetic data with one-minute resolution from the Entoto station was used to determine the horizontal magnetic field
- strength. The observed horizontal magnetic field strength, $H_{\rm obs}$, was computed from the orthogonal magnetic field components
- 186 X and Y as:

187
$$H_{\rm obs} = \sqrt{X^2 + Y^2}$$
. (1)

188 3.3 Internal Field Removal

- 189 To account for the Earth's internal field, we used the CHAOS geomagnetic field model (Finlay et al., 2020) to estimate the
- internal horizontal field, $H_{\rm int}$, at the station's geographic location and for each observation time. The residual horizontal field
- 191 was obtained by subtracting the internal field:

192
$$H_{\rm res} = H_{\rm obs} - H_{\rm int}$$
. (2)

193 This residual field contains contributions from both ionospheric and magnetospheric sources.

194 3.4 Equatorial Electrojet Signal Extraction

- To isolate the ionospheric EEJ signal, we selected the $H_{\rm res}$ values corresponding to local daytime hours, typically from 09:00
- 196 to 15:00 LT, when EEJ activity is strongest (Onwumechili, 1997a; Rangarajan et al., 2002). This subset of the residual field
- 197 represents the unrefined EEJ signal.

198 3.5 Magnetospheric Contribution Isolation

- 199 The nighttime portion of the residual field, spanning 18:00 to 06:00 LT, is assumed to be dominated by magnetospheric
- 200 contributions due to the absence of significant ionospheric currents. This signal was extracted and analyzed alongside the
- 201 global Dst index (Sugiura, 1964) to assess their correlation, which will be discussed in more detail in the Results section.
- To assess the capability of the Entoto station to detect space weather effects, we generated a time series comparing the local
- 203 magnetospheric signal, extracted from nighttime residuals of the horizontal magnetic field, with the global Dst index. Then
- we selected geomagnetically quiet periods (Dst > -20) and disturbed periods (Dst < -50) in order to show superposed epoch
- 205 plots of the EEJ signal, showing its diurnal variation averaged over each period. The first method will illustrate the station's
- 206 sensitivity to global magnetospheric conditions, while the second will show how ionospheric currents (particularly the EEJ)
- 207 behave during quiet and disturbed times. To support this visual analysis, we will also perform two quantitative comparisons:
- a Pearson correlation between the magnetospheric signal as measured at the station and Dst to measure the linear association,





and a comparison of the mean daily maximum EEJ amplitude during quiet and storm conditions. These metrics provide a simple statistical measure of the station's physical response to varying levels of geomagnetic activity.

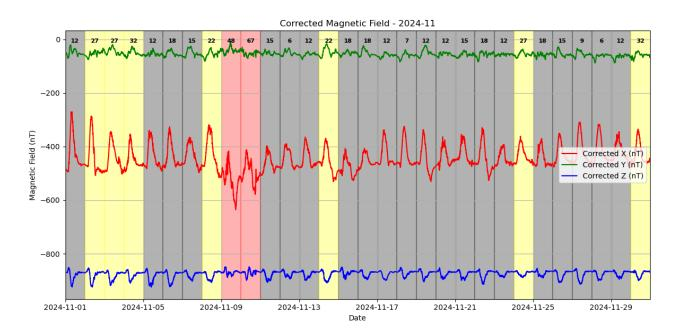


Figure 3. Variations in the local geomagnetic field along the X (red line), Y (green line), and Z (blue line) components during November 2024. At the top of the graph the daily maximum Ap value is shown. The greyed out days refer to quiet times, yellow days are unsettled, and red is disturbed days.

211 4 Results and Discussion

212

213

214

215216

217

218

219220

221

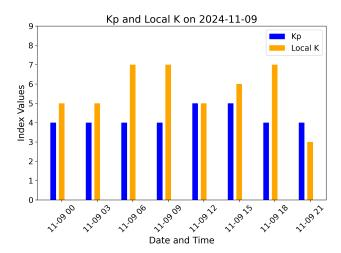
222

The processed diurnal variations were visualized by plotting the residual components $\Delta X, \Delta Y, \Delta Z$ against local time to observe the daily geomagnetic patterns. Plots were generated for each complete month since deployment until January 2025 as shown in Figures 3, 5, and 7. Additionally, solar activity indices, including the Ap index, were compared with the diurnal variations to evaluate the influence of solar activity on the geomagnetic field. Based on the Ap-index values, the above analyses show that the geomagnetic field variations were consistent with the planetary geomagnetic activity levels. During the night, the fields were generally stable for quiet days. When the geomagnetic activity was high, irregular variations were detected during both daytime and nighttime.

The comparison between the global planetary Kp index and the locally derived K index at the Entoto station consistently shows that the local K values are approximately one to two levels higher, even during geomagnetically quiet periods, shown for selected times in Figures 4 and 6. This discrepancy can largely be attributed to the station's location near the magnetic equator, where it is strongly influenced by the Equatorial Electrojet (EEJ). The EEJ introduces pronounced diurnal variations







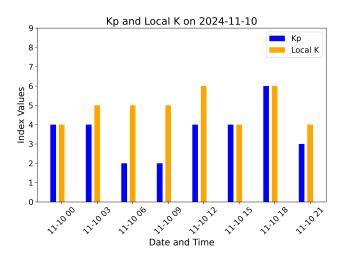


Figure 4. Kp and local K indices derived from the Entoto station. Both figures show indices as measured during disturbed storm times, as seen in Figure 3.

in the horizontal component of the geomagnetic field, which are not captured in the mid-latitude stations contributing to the Kp index (Forbes and Lindzen, 1981; Onwumechili, 1997b). Consequently, the Entoto station records elevated field disturbances relative to global averages.

In the present study, a historical K9 threshold value of 242 nT, derived from the former AAE INTERMAGNET observatory in Addis Ababa (latitude 9.035° N, longitude 38.77° E), was used to calculate the local K index. However, the significance of this threshold is limited by the fact that the observatory was located at a geomagnetic latitude of less than 10° , where the EEJ strongly modulates magnetic variability and distorts comparisons with mid-latitude standards. As such, this K9 value may not adequately characterize the magnetospheric and ionospheric influences at low-latitude sites like Entoto. As part of future work, a dedicated and empirically determined L_9 value will be established for Entoto once a longer time series of high-quality data becomes available (Menvielle et al., 1995; Korte et al., 2018).

Figures 8, 9, and 10 show the measured magnetospheric signal of the station versus the global Dst index, the EEJ signal during quiet (Dst > -20), and disturbed (Dst < -50) times respectively. These Figures illustrate the ability of the Entoto station to capture both magnetospheric and ionospheric responses to space weather conditions. Figure 8 demonstrates a moderate to strong Pearson correlation of 0.62 between the station's derived magnetospheric signal and the global Dst index, indicating that the station reliably reflects variations in magnetospheric current systems. Figures 9 and 10 compare the equatorial electrojet (EEJ) signal during geomagnetically quiet and disturbed periods. The mean daily maximum EEJ amplitude was significantly larger during storm days (-317.9 nT) than during quiet days (-257.2 nT), suggesting that the station effectively captures enhancements in the EEJ associated with storm-time ionospheric dynamics. These preliminary results confirm the station's sensitivity to both global geomagnetic disturbances and regional ionospheric variability.





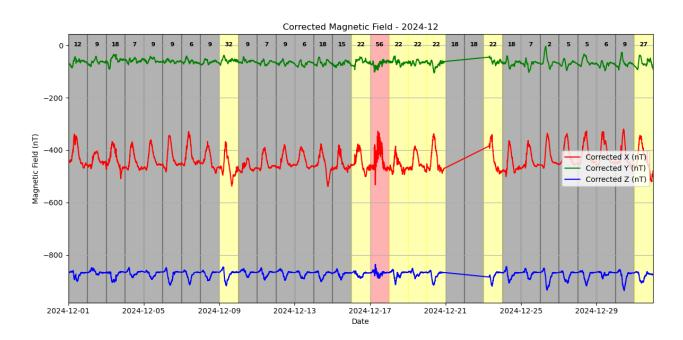


Figure 5. Variations in the local geomagnetic field along the X (red line), Y (green line), and Z (blue line) components during December 2024. As described in Figure 3

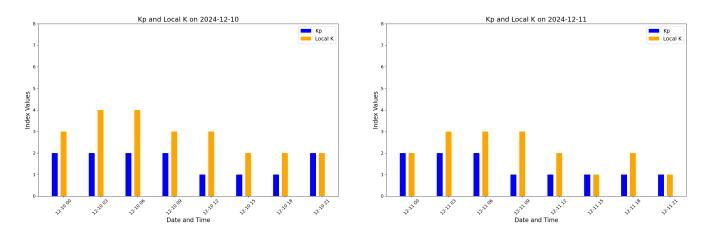


Figure 6. Kp and local K indices derived from the Entoto station. Here Figures show indices during quiet times, as seen in Figure 5.





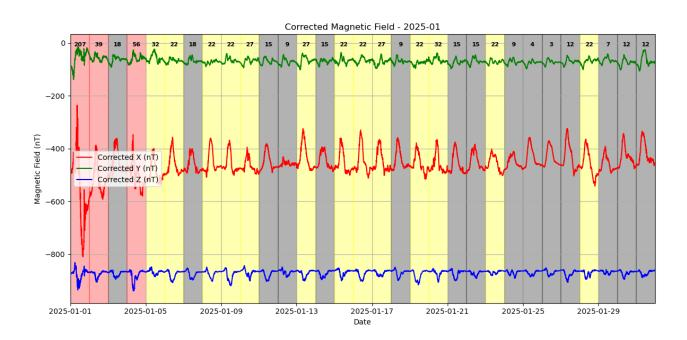


Figure 7. Variations in the local geomagnetic field along the X (red line), Y (green line), and Z (blue line) components during January 2025. As described in Figure 3

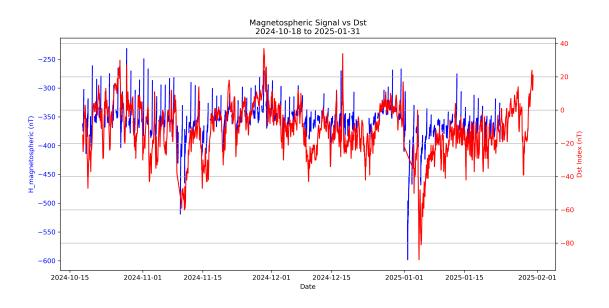


Figure 8. The measured magnetospheric signal of the station versus the global Dst index for date range 2024-10-18 to 2025-01-31





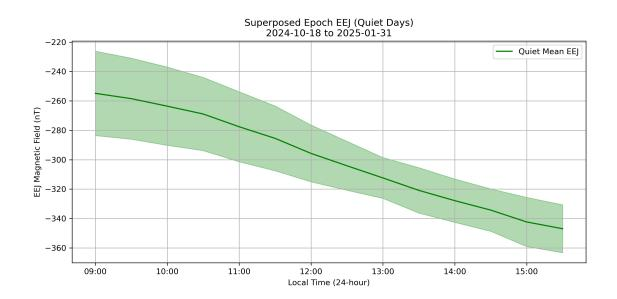


Figure 9. The superposed EEJ signal during quiet (Dst > -20) times for the date range 2024-10-18 to 2025-01-31

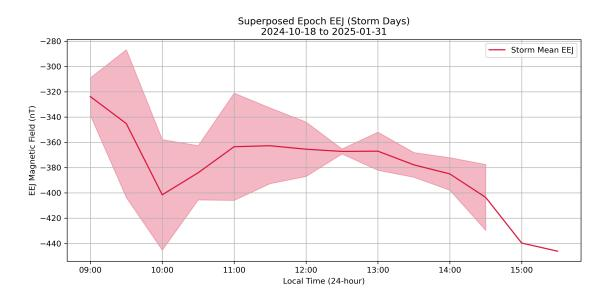


Figure 10. The superposed EEJ signal during storm (Dst < -50) times for the date range 2024-10-18 to 2025-01-31





Conclusion

242

247 248

249

250 251

252 253

254 255

256

257

258 259

260 261

262 263

264 265

266 267

273

274

275

Variations in the local geomagnetic field along the X, Y, and Z components were plotted alongside the maximum daily Ap 243 244 values. This was used to identify recurring patterns and assessing the impact of space weather over extended periods. This preliminary data from the Entoto Magnetometer Station shows clear variations in the geomagnetic field, particularly during 245

periods of increased solar activity. 246

> The local K-index for the Entoto station was estimated using the MagPy software and compared against the planetary Kindex. These results are consistent with previous studies (Kotzé et al., 2015), which have demonstrated the value of the local K-index in assessing geomagnetic activity, particularly in regions with distinctive geomagnetic features. In the case of Entoto, situated near the magnetic equator, the influence of the equatorial electrojet (EEJ) plays a significant role. As expected, the local K-index was typically higher than the planetary K-index, both during quiet and disturbed periods. This discrepancy underscores the importance of generating a station-specific L9 (K9 lower limit) value once sufficient data has been collected. While this would improve the precision of the local K-index, determining an appropriate L9 value in equatorial regions is inherently challenging due to the dynamic and variable nature of the EEJ.

> Despite these challenges, further analysis across several geomagnetic storms revealed prompt increases across all field components, confirming the station's responsiveness to magnetospheric disturbances. The performance of the local K-index, though influenced by EEJ effects, demonstrates Entoto's capability to provide meaningful space weather data, aligning with methods applied in other equatorial observatories (Myint et al., 2022). The combination of CHAOS 8.2 internal and external field corrections, high-pass filtering, and preliminary regional K-index estimation forms a framework for interpreting magnetic field variations at this station, and creates a foundation for future upgrades.

> Initial results demonstrate the station's ability to detect and characterize geomagnetic disturbances, with observed field changes aligning well with Dst index variations. The correlation between magnetospheric signals and global disturbance indices suggests that the Entoto station is sensitive to space weather drivers, hence proves useful for regional monitoring.

> As the only current equatorial observatory on the African continent, the Entoto Magnetometer Station plays a critical role in addressing current gaps in longitudinal geomagnetic data. Its location on the magnetic equator enables detailed observations of equatorial ionospheric phenomena, including the Equatorial Electrojet (EEJ) and Sq currents, which are poorly resolved by mid- and high-latitude stations.

The computation of a local K-index using a historical L₉ threshold of 242 nT, based on the former AAE magnetic observatory 268 15 kilometres away from the newly deployed station, highlights both the value and limitations of such metrics in equatorial 269 regions. While the local K-index was consistently higher than the global Kp, this discrepancy, also observed in other studies 270 271 (Myint et al., 2022), underscores the need to determine a site-specific L₉ value for Entoto. However, the day-to-day variability 272 introduced by the EEJ makes this a challenging task.

The comparison between the station's magnetospheric signal and the Dst index, along with the observed differences in EEJ amplitude during quiet and disturbed periods, highlights the capability of the Entoto Magnetometer Station to capture both global and regional geomagnetic variations.





So despite some challenges, the observed responses to geomagnetic storms, the correlation with Dst, and the strong performance of the preliminary K-index estimation all confirm the Entoto station's potential to deliver accurate and valuable space weather measurements. These results mark an important milestone for geomagnetic monitoring in Africa and demonstrate the station's readiness to contribute to the global geomagnetic observatory network.

6 Future Work

280

- While the initial results have focused on geomagnetic field variations, future studies will expand to include a deeper analysis
- 282 of ionospheric effects, such as the Equatorial Electrojet (EEJ) and Sq variations. These phenomena are of particular interest for
- 283 understanding how space weather affects the African sector. It is also imperative to calculate a local L9 value. Additionally,
- 284 there is potential for expanding the network of magnetometer stations across Africa to improve longitudinal data coverage.
- 285 The deployment of the Entoto Magnetometer Station marks a significant milestone in geomagnetic monitoring in the African
- 286 region. The initial results show that the station is well-equipped to contribute valuable data to global space weather research.
- 287 With future expansions and collaborations, this station will play an increasingly important role in understanding geomagnetic
- 288 and ionospheric phenomena in this critical region.

289 Author Contribution

- 290 AN, NG, ZI, and DC were responsible for the deployment of the Entoto station. MS, OB, and JM contributed to the processing
- 291 of raw data into IAGA format and supported the development and operation of the data transfer software. AN performed the
- 292 data analysis and drafted the results and conclusions sections.

293 Competing Interests

294 The authors declare that there are no competing interests.

295 Data Availability

- 296 The data from the Entoto Magnetometer Station will be made available to the scientific community for non-commercial re-
- 297 search purposes upon reasonable request to the corresponding author.
- 298 Acknowledgements. The authors would like to acknowledge Leonhardt Roman for developing and maintaining the MagPy software suite,
- 299 which was instrumental in processing and analyzing magnetic field data for this study. We thank Chane Moges and Yekoye Tariku for
- 300 their assistance during the deployment of the magnetometer. We also extend our sincere thanks to Emmanuel Nahayo at the South African
- 301 National Space Agency (SANSA) for his support in assessing the preliminary geomagnetic measurements from the Entoto station. Also Oliver
- 302 **Bronkala** of the GFZ who assisted in transferring the data to a dedicated server.





for Geosciences in Potsdam.

The Entoto dual magnetometer station is operated with the support of the Entoto Observatory and Research Center, with technical collaboration from SANSA and GFZ Potsdam. We also acknowledge the INTERMAGNET network and its data standards, which served as a reference framework during quality assurance.

This research made extensive use of open-source tools, including Python, pandas, matplotlib, and SciPy, and we gratefully acknowledge the open-science community for their contributions. The author(s) acknowledge the use of the AI language model ChatGPT for

assistance with Python syntax correction and Grammarly for language refinement in the preparation of this manuscript.

We acknowledge the use of the *CHAOS* geomagnetic field model, developed and maintained by the *Technical University of Denmark* (*DTU*), which was used to remove field contributions from the observations. We further acknowledge the providers of geomagnetic indices:

the Dst index supplied by the World Data Center for Geomagnetism, Kyoto, and the Ap index provided by the GFZ German Research Centre





313 References

- Denardini, C. M., da Silva, M. R., Gende, M. A., Chen, S. S., Fagundes, P. R., Schuch, N. J., Petry, A., Resende, L. C. A., Moro, J., Padilha,
- A. L., Sant' Anna, N., and Alves, L. R. (2015). The initial steps for developing the south american k index from the embrace magnetometer
- 316 network. Revista Brasileira de Geofísica, 33(1):79–88.
- 317 Finlay, C. C., Kloss, C., Olsen, N., Hammer, M. D., Tøffner-Clausen, L., Grayver, A. V., and Kuvshinov, A. (2020). The chaos-7 geomagnetic
- field model and observed changes in the south atlantic anomaly. Earth, Planets and Space, 72(1):156.
- 319 Forbes, J. M. and Lindzen, R. S. (1981). Solar semidiurnal tide in the thermosphere. Journal of Atmospheric and Terrestrial Physics,
- 320 43(5-6):407-413.
- 321 Giday, N. M., Katamzi-Joseph, Z. T., and Stoneback, R. (2020). Effect of moderate geomagnetic storms on equatorial plasma bubbles over
- astern africa in the year 2012: Evolution and electrodynamics. Advances in Space Research, 65(7):1701–1713.
- 323 Habarulema, J. B., Lefebvre, G., Moldwin, M. B., Katamzi-Joseph, Z. T., and Yizengaw, E. (2019). Counter-electrojet occurrence as observed
- from c/nofs satellite and ground-based magnetometer data over the african and american sectors. Space Weather, 17(7):1090–1104.
- 325 Hamid, N. S. A., Liu, H., Uozumi, T., Yumoto, K., Veenadhari, B., Yoshikawa, A., and Sanchez, J. A. (2014). Relationship between the
- equatorial electrojet and global sq currents at the dip equator region. Earth, Planets and Space, 66(1):146. Received: 31 March 2014;
- 327 Accepted: 16 October 2014; Published: 29 October 2014.
- 328 Kamide, Y. (2001). Geomagnetic Storms as a Dominant Component of Space Weather: Classic Picture and Recent Issues, pages 43-77.
- 329 Springer Netherlands, Dordrecht.
- 330 Kloss, C., Finlay, C. C., Olsen, N., Tøffner-Clausen, L., Gillet, N., and Grayver, A. (2025). Chaos-8.2 geomagnetic field model.
- 331 Korte, M., Mandea, M., Kotzé, P., and Menvielle, M. (2018). The geomagnetic observatory network and its evolution. *Annales Geophysicae*,
- 332 36:1327–1343.
- 333 Kotzé, P. B., Cilliers, P. J., and Sutcliffe, P. R. (2015). The role of sansa's geomagnetic observation network in space weather monitoring: A
- 334 review. Space Weather, 13(10):656-664.
- 335 Macmillan, S. (2007). Observatories: an overview. Springer.
- 336 Matzka, J., Chulliat, A., Mandea, M., Finlay, C. C., and Qamili, E. (2010). Geomagnetic observations for main field studies: From ground to
- 337 space. Space Science Reviews, 155(1-4):29–64.
- 338 Menvielle, M., Papitashvili, N., Häkkinen, L., and Sucksdorff, C. (1995). Computer production of k indices: review and comparison of
- methods. Geophysical Journal International, 123(3):866–886.
- 340 Mungufeni, P., Habarulema, J. B., Migoya-Orué, Y., and Jurua, E. (2018). Statistical analysis of the correlation between the equatorial
- electrojet and the occurrence of the equatorial ionisation anomaly over the east african sector. *Annales Geophysicae*, 36(3):841–853.
- 342 Myint, L. M., Hozumi, K., Saito, S., and Supnithi, P. (2022). Analysis of local geomagnetic index under the influence of equatorial electrojet
- 343 (eej) at the equatorial phuket geomagnetic station in thailand. Advances in Space Research, 70(5):1429–1440.
- Nel, A. E. and Kotzé, P. B. (2024). A comparative investigation of geomagnetic jerks across the saa during the period 2000–2020. Geophysical
- 345 *Journal International*, 239(1):192–200.
- 346 Nel, A. E., Morschhauser, A., Vervelidou, F., and Matzka, J. (2024). A new high-resolution geomagnetic field model for southern africa.
- 347 South African Journal of Science, 120(1/2).
- 348 Onwumechili, C. A. (1997a). The Equatorial Electrojet. Gordon and Breach Science Publishers.
- 349 Onwumechili, C. A. (1997b). The Equatorial Electrojet. Gordon and Breach Science Publishers, Amsterdam.





- 350 Rangarajan, G. K., Iyemori, T., and Yumoto, K. (2002). Estimation of sq and eej currents and their seasonal variation using ground-based
- magnetic data. Earth, Planets and Space, 54(5):527–538.
- 352 Stolle, C., Michaelis, I., and Reda, J. (2018). MagPy Magnetometer Python Toolbox.
- 353 Sucksdorff, C., Pirjola, R., and Häkkinen, L. (1991). Computer production of k-indices based on linear elimination. Geophysical Transac-
- 354 *tions*, 36(3-4):335–345.
- 355 Sugiura, M. (1964). Hourly values of equatorial dst for the igy. Annals of the International Geophysical Year, 35:9–45.
- 356 Uemoto, J., Maruyama, T., Saito, S., Ishii, M., and Yoshimura, R. (2010). Relationships between pre-sunset electrojet strength, pre-reversal
- enhancement and equatorial spread-f onset. *Annales Geophysicae*, 28(2):449–454.
- 358 Yamazaki, Y. and Maute, A. (2016). Sq and eej—a review on the daily variation of the geomagnetic field caused by ionospheric dynamo
- 359 currents. Space Science Reviews, 201(1-4):1–186.
- 360 Yizengaw, E. and Moldwin, M. B. (2009). African meridian b-field education and research (amber) array. Earth, Moon, and Planets,
- 361 104(1-4):237–246.